On the Interdiffusion-Based Quantum Cascade Laser

Saša Kočinac, Stanko Tomić, Zoran Ikonić, and Vitomir Milanović

***Abstract*—Design procedure for the active region of current pumped quantum cascade laser is proposed, so to achieve maximal gain. Starting with an arbitrary smooth potential, a family of isospectral Hamiltonians with predefined energy spectrum is generated using the inverse spectral theory. By varying the relevant control parameter the potential shape is varied, inducing changes in transition dipole moments and electron–phonon scattering times, and the optimal potential which gives the largest gain is thus found. For purpose of realization, a simple step quantum-well structure with just a few layers is then designed so that in the post-growth heating-induced layer interdiffusion, it will acquire a shape as close as possible to the optimal smooth potential.**

***Index Terms*—Gain optimization, layer interdiffusion, quantum cascade lasers.**

I. Introduction

FOLLOWING the seminal paper [1] by Kazarinov and Suris, who proposed lasing based on intersubband transitions in biased quantum wells (QW), and the first demonstration of lasing by Faist *et al.* [2], who employed a strain-free InGaAs–AlInAs periodic structure, lattice matched to InP, to realize the quantum cascade laser (QCL), a significant progress has been made in covering a wide spectral range of emission wavelengths 4–20 μm [3]. The main task in the design of unipolar QW lasers (either electrically or optically pumped [4]) is to maximize the gain.

In this letter, we develop a procedure for realization of optimal QW profile by first designing a comparatively simple structure with just a few layers at the time of growth, which would in the next, post-growth processing step—the heat treatment induced layer interdiffusion—acquire the approximately optimal smooth shape derived by inverse spectral theory (IST) [5]. We focus the analysis on electrically pumped three-level AlGaAs QCL based on vertical transitions [6]. These have a smaller sensitivity to interface roughness than the diagonal transition QCLs, and hence, a narrower gain spectrum and lower threshold.

For comparative analysis of various structures, it is reasonable to consider modal gain G_m, rather than gain $g = G_m/L_W$ (where L_W is the effective width of the structure), otherwise incorrect conclusions may be obtained [7]. In current pumped laser this is given by

$$G_m = \frac{4\pi e}{\tilde{n}\varepsilon_0 \lambda 2\Gamma} z_{32}^2 \tau_3 \left(1 - \frac{\tau_{21}}{\tau_{32}}\right) \cdot J \tag{1}$$

where J is the injection current density, e the electron charge, ε_0 the vacuum permittivity, $\tilde{n}$ is the modal refractive index, λ the emission wavelength, $z_{32} = \langle 3|z|2\rangle$ the dipole matrix element of the lasing transition, and 2Γ is the luminescence linewidth [full-width at half maximum (FWHM)]. The lifetimes of laser levels are $1/\tau_2 = 1/\tau_{21} + 1/\tau_{23} \approx 1/\tau_{21}$ and $1/\tau_3 = 1/\tau_{31} + 1/\tau_{32}$, where $1/\tau_{ij}$ denotes the sum of optical and acoustic phonon scattering rates. The gain maximization problem is thus to find the QW profile which maximizes the target function

$$\Xi = z_{32}^2 \tau_3 \left(1 - \frac{\tau_{21}}{\tau_{32}}\right). \tag{2}$$

Each term in Ξ depends on the wavefunctions involved, and the scattering times also depend on state energies. They also depend to some extent on the temperature and electron density, but this dependence is not very strong and will here be neglected, to avoid having the case-specific optimization. Concerning the energies, there are some constraints imposed from the outset, which make the state energies fixed, rather than variable quantities. The spacing between the upper and lower laser state is fully fixed by the lasing wavelength, and the spacing between the lower laser and the ground state is essentially fixed to be equal to longitudinal optical (LO) phonon energy, because this choice provides the fastest relaxation (i.e., emptying) of the lower laser state. Generally, there may exist special circumstances where one would want to relax the latter condition, e.g., shifting the lower laser state away from the ground state may sometimes suppress electrons backfilling it, with a favorable overall effect. However, such subtleties would require more complicated considerations of both the active and injector regions of QCL, which is not the subject of this work. Therefore, we consider state energies to be fixed, and the parameter Ξ may then be varied by changing the QW potential shape in isospectral manner, which affects only the wavefunctions and not state energies.

To perform the gain maximization, we have used in the first phase the procedure described in [5]. The IST based potential variation comprises two steps, first we manipulate a chosen initial potential by appropriately positioning its bound states. With the initial potential taken as Pöschl–Teller (PT) potential, this is done by varying its parameters s and a [5]. The convenience of the PT potential is that its eigenenergies are known analytically. This allows one to simply set the spacing of two states, e.g., $|3\rangle$ and $|1\rangle$, to a desired value, by choosing an appropriate value of

Manuscript received February 4, 2002; revised April 17, 2002.

S. Kočinac is with the Faculty of Technology and Metallurgy, University of Belgrade, 11000 Belgrade, Yugoslavia.

S. Tomić is with the Department of Physics, University of Surrey, Guildford, GU2 7XH Surrey, U.K. (e-mail: s.tomic@surrey.ac.uk).

Z. Ikonić is with the School of Electronic and Electrical Engineering, University of Leeds, LS2 9JT Leeds, U.K.

V. Milanović is with the Faculty of Electrical Engineering, University of Belgrade, 11000 Belgrade, Yugoslavia.

Publisher Item Identifier S 1041-1135(02)06025-1.

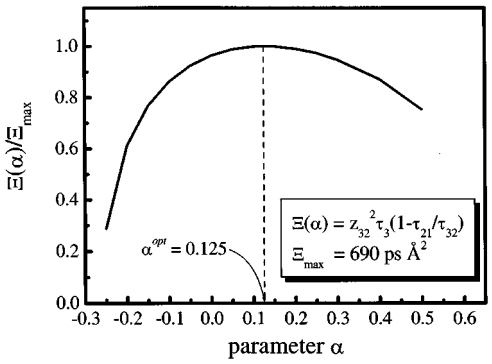

Fig. 1. The normalized value of parameter $\Xi(\alpha)/\Xi_{\max}$, which determines the laser gain as it depends on the IST-parameter α for $s^{\rm opt} = 5.4$ (in the PT potential) calculated for $\Delta E_{31} = 152$ meV. The maximal value of Ξ is obtained for $\alpha^{\rm opt} = 0.125$.

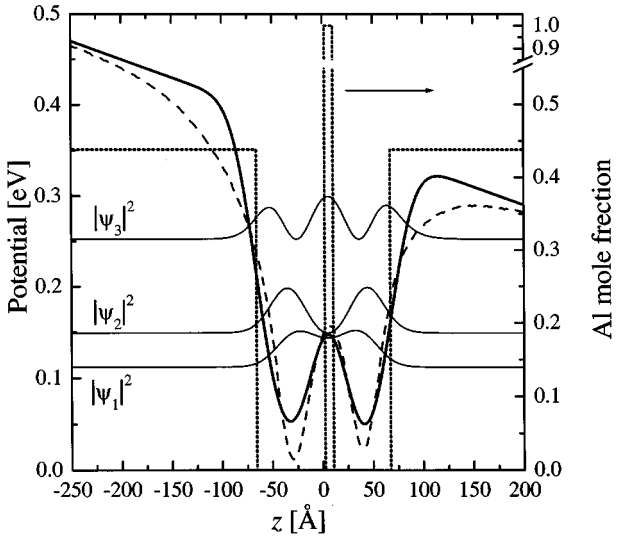

Fig. 2. The IST-optimized (dashed) and interdiffusion-generated (solid) potential with $K_0 = 40$ kV/cm bias included, and the wavefunctions of the three relevant states in the interdiffused QW.

the parameter a for any specified value of the (free) parameter s. Then, using the IST a whole family of isospectral potentials of different shapes, controlled by the IST parameter α, is generated. Here, we have required $\Delta E_{31} = 152$ meV which, after shifting the lower lasing level $|2\rangle$ by the IST formalism so that ΔE_{21} becomes resonant with the LO phonon energy (36 meV in AlGaAs), will deliver the lasing wavelength of 10.6 μm. A family of potentials $U^{\rm IST}\{z, \alpha, V_{\rm PT}(s)\}$ is thus formed, all of them having the same $\Delta E_{21} = 36$ meV and $\Delta E_{32} = 116$ meV. Thus, with the potential shape controlled by the (isospectral) IST parameter α and the external-to-IST parameter s, we have a considerably expanded "range" of explored potentials, as compared to applying the IST alone to a fully fixed initial potential.

At this point, we recall that QCL structure is biased, and a part of the potential generated by any particular choice of s and α in fact originates from the electric field, the rest being due to the material composition grading. We have here assumed a "typical" value $K_0 = 40$ kV/cm, i.e., the corresponding linear potential is subtracted from the currently considered potential in order to get the part to be realized by composition grading. This part, however, is valid within the constant effective mass model, so we use the coordinate transform method to generate the potential consistent with the effective mass variation, as described in [8]. In evaluating the target function (2), we include the nonparabolicity, as described in [9]. It should be noted that the nonparabolicity (which cannot be embedded in the IST-procedure itself) slightly changes the state energies, and this is compensated for by slightly detuning the initially chosen state energies, within the parabolic model, from the actually required values. By repeating this procedure across the two-dimensional (α, s) space of free parameters, the set that maximizes the target function is spotted (Fig. 1). In this example, the maximum was found to occur at $\alpha = 0.125$ and $s = 5.4$, from which the necessary grading is derived. This IST-optimized potential, with the bias included, is shown in Fig. 2. The full potential (i.e., its central part) is almost symmetric, while the bias-free, gradient-induced part of it clearly is not. This feature of the optimal QCL potential is consistent with the form of the target function (2), and is in sharp contrast to the situation in optically pumped lasers, where the optimal potential necessarily has to be quite asymmetric [5].

The derived smooth potential profiles may in principle be realized by directly modulating the alloy composition at time of structure growth, but this is not very practical. An alternative route to approximate realization of the optimal potential is to start with a structure which has a small number of layers and use interdiffusion. In course of post-growth heat treatment of (typically) initially stepwise-constant QW structures, the constituent materials diffuse toward smoothed profiles, hence changing the potential, wavefunctions, and energies. This technique has been successfully employed for tuning the wavelength of AlGaAs-based intersubband infrared photodetectors [10]. Here, we employ this technique to generate QW profiles approximating those derived as optimal for the laser.

Consider a structure made of N layers of $\mathrm{Al}_x\mathrm{Ga}_{1-x}\mathrm{As}$ with Al mole fraction in jth layer denoted as x_j (constant within a layer), embedded in bulk of the composition x_0 on the left and x_{N+1} on the right of the multilayer stack. In a specified coordinate system, the left boundary of jth layer is denoted as z_{j-1}, and the right boundary as z_j (i.e., the width of jth layer is $z_j - z_{j-1}$). Starting with this stepwise-constant profile, due to the interdiffusion by thermal annealing at constant temperature, the profile will change in time according to [10], [11]

$$x(z,t) = \sum_{j=1}^{N} \frac{x_j}{2}\left[\mathrm{Erf}\left(\frac{z-z_{j-1}}{L_d}\right) - \mathrm{Erf}\left(\frac{z-z_j}{L_d}\right)\right] + \frac{x_0}{2}\left[1 - \mathrm{Erf}\left(\frac{z-z_0}{L_d}\right)\right] + \frac{x_{N+1}}{2}\left[1 + \mathrm{Erf}\left(\frac{z-z_N}{L_d}\right)\right] \quad (3)$$

where $L_d = 2\sqrt{Dt}$ is the diffusion length, D is the diffusion coefficient, which depends on the annealing temperature (and is well known for the AlGaAs system [11]), and t the annealing time. Note that the influence of temperature (via the coefficient D) and of time is in case of AlGaAs system grouped into a single parameter L_d, but in, e.g., 4-component systems, these would come in independently. One then has the task to design the initial structure (the widths and compositions of inner layers) so that

TABLE I
DIPOLE MATRIX ELEMENT z_{32} IN [Å], RELAXATION TIMES τ_{ij} IN [ps], AND THE FIGURE OF MERIT Ξ IN [psÅ^2] FOR THE IST-OPTIMIZED AND 3-LAYER INTERDIFFUSED STRUCTURES

	z_{32}	τ_{21}	τ_{31}	τ_{32}	τ_3	Ξ
IST	26.5	0.22	2.26	2.19	1.11	690
Diff.	29.3	0.22	1.77	1.63	0.85	630

after interdiffusion specified by an additional free parameter L_d, the resulting profile $x(z, t)$ is as close as possible to the desired $x_{\text{target}}(z)$. For an N-layer structure there are, thus $2N+1$ free parameters, while the bulk compositions on the left and right are actually fixed by $x_{\text{target}}(z)$ itself. For finite N it is generally impossible to get full coincidence of the two profiles, but fairly good agreements may be obtained by fitting.

To design a suitable initial N-layer structure we employ the simulated annealing algorithm [12]. It varies all $2N+1$ structural parameters, uses them in (3), compares the interdiffused profile with the target, IST-optimized profile, and minimizes the mean square deviation between the two. We have thus designed a structure with just $N = 3$ inner layers, which after interdiffusion, reproduces the optimal potential reasonably well. Its parameters are: GaAs (67.91 Å $=$ 24 m.l.)—AlAs (8.49 Å $=$ 3 m.l.)—GaAs (56.6 Å $=$ 20 m.l.)—embedded in $Al_{0.438}Ga_{0.562}As$ outer barriers bulk, and after interdiffusion characterized by $1/L_d = 0.0365$ Å^{-1} it will deliver the profile maximally similar to the target, IST-optimized profile, both also being shown with the bias field present in Fig. 2. Even better fits are obtainable with larger N, but the simplicity of the 3-layer structure to be initially grown is a very attractive feature. Checking various relevant quantities corresponding to the interdiffused profile shows that it is still acceptable: the state spacings now amount to $\Delta E_{32} = 103.4$ meV and $\Delta E_{21} = 37.2$ meV, while the relevant relaxation times and matrix elements are given in Table I, together with the values corresponding to the IST-optimized well. The resulting gain parameter $\Xi = 630$ psÅ^2 is indeed somewhat lower than 690 psÅ^2 predicted for the IST-optimized potential, though the decrease is tolerable. Some difference might have been expected, because the IST-optimized well has quite different slopes of composition near the well bottom and barrier top, with characteristic length scales of 30–50 Å and ~150 Å, respectively, which cannot both be accurately reproduced by a linear combination of the same set of Erf functions.

Finally, we should point to some problems one may encounter in the interdiffusion based QCL realization: the heat treatment also induces dopants diffusion, and the current QCL designs rely *inter alia* on having the doped layers remote from the active region. Using the $D(T) = D_0 \exp(-E_a/kT)$ scaling of the diffusion constants with temperature T one may try to find conditions where the (usually faster) dopant diffusion can be kept at bay. With the published values of parameters for Si dopants in GaAs ($E_a = 0.90$ eV, $D_0 = 3.6 \times 10^{-11}$ cm^2/s [13]) and for GaAs–AlAs interdiffusion ($E_a = 6$ eV, $D_0 = 2.4 \times 10^8$ cm^2/s [11]) we find that the process temperature should be $\geq$1085 °C in order to have the dopants diffusion slower than interdiffusion. The QCLs usually have 40–150-Å wide doped regions, spaced by 50–250 Å from the active region, so the dopants spreading equal to the above stated (optimal) interdiffusion value of $L_d \approx 28$ Å should be acceptable. Therefore, the interdiffusion should be performed at high, though still realistic temperatures.

In conclusion, a design procedure for the active region of QCL is proposed, which relies on layer interdiffusion in a simple step QW structure to approximately realize the theoretically derived optimal smooth profile. Comparison with a few other structures [6], [14] shows an improvement of the gain parameter by at least 40% is achieved in the present design, making it potentially useful in QCL fabrication.

REFERENCES

[1] R. F. Kazarinov and R. A. Suris, "Possibility of the amplification of electromagnetic waves in a semiconductor with superlattice," *Sov. Phys. Semicond.*, vol. 5, pp. 707–711, 1971.

[2] J. Faist, F. Capasso, D. L. Sivco, C. Sirtori, A. L. Hutchinson, and A. Y. Cho, "Quantum cascade laser," *Science*, vol. 264, pp. 553–556, 1994.

[3] F. Capasso, C. Gmachl, R. Paiella, A. Tredicucci, A. L. Hutchinson, D. L. Sivco, J. N. Baillargeon, A. Y. Cho, and H. C. Liu, "New frontiers in quantum cascade lasers and applications," *IEEE J. Select. Topics Quantum. Electron.*, vol. 6, pp. 931–947, Nov.–Dec. 2000.

[4] J. Wang, J.-P. Leburton, F. H. Julien, and A. Saar, "Design and performance optimization of optically-pumped mid-infrared intersubband semiconductor lasers," *IEEE Photon. Technol. Lett.*, vol. 8, pp. 1001–1003, Aug. 1996.

[5] S. Tomić, M. Tadić, V. Milanović, and Z. Ikonić, "The optimization of optical gain in the intersubband quantum well laser," *J. Appl. Phys.*, vol. 87, p. 7965, 2000.

[6] C. Sirtori, P. Kruck, S. Barbieri, P. Collot, J. Nagle, M. Beck, J. Faist, and U. Oesterle, "GaAs/AlGaAs quantum cascade lasers," *Appl. Phys. Lett.*, vol. 73, pp. 3486–3488, 1998.

[7] P. Blood, "On the dimensionality of optical absorption, gain and recombination in quantum-confined structures," *IEEE J. Quantum Electron.*, vol. 36, pp. 354–362, Mar. 2000.

[8] V. Milanović and Z. Ikonić, "Equispaced-level Hamiltonians with the variable effective mass following the potential," *Phys. Rev. B*, vol. 54, pp. 1998–2003, 1996.

[9] C. Sirtori, F. Capasso, and J. Faist, "Nonparabolicity and a sum rule associated with bound-to-bound and bound-to-continuum intersubband transitions in quantum wells," *Phys. Rev. B*, vol. 50, pp. 8663–8674, 1994.

[10] X. Liu *et al.*, "Wavelength tuning of GaAs/AlGaAs quantum-well infrared photodetectors by thermal interdiffusion," *Jpn. J. Appl. Phys.*, vol. 38, pp. 5044–5046, 1999.

[11] T. E. Schlesinger and T. Kuech, "Determination of the interdiffusion of Al and Ga in undoped (Al,Ga)As/GaAs quantum wells," *Appl. Phys. Lett.*, vol. 49, pp. 519–521, 1986.

[12] A. Corana, M. Marchesi, C. Martini, and S. Ridella, "Minimizing multimodal functions of continuous variables with the 'simulated annealing' algorithm," *ACM Trans. Math. Softw.*, vol. 13, pp. 262–280, 1987. [Online]. Available: http://www.netlib.org/opt/simann.f, (the Fortran code).

[13] J. E. Cunningham, T. H. Chiu, W. Jan, and T. Y. Quo, "Nonlinear dependencies of Si diffusion in δ-doped GaAs," *Appl. Phys. Lett.*, vol. 59, pp. 1452–1454, 1991.

[14] P. Kruck, H. Page, C. Sirtori, S. Barbieri, M. Stellmacher, and J. Nagle, "Improved temperature performance of $Al_{0.33}Ga_{0.67}As$/GaAs quantum-cascade lasers with emission wavelength at $\lambda \approx 11\mu$m," *Appl. Phys. Lett.*, vol. 76, pp. 3340–3342, 2000.